Supplementary Information (SI) for RSC Advances.

Efficient Regeneration of Pd-SSZ-13 catalysts deactivated by alkali metals for Passive NO_x Adsorption

Dongdong Chen[a, b, *], Weiqi Zhang[a], Zhenzhen Jia[a], Huibin Liu[b], Bo Zhang[a], Shasha Liu[a], Feng Liang[a], Wuwan Xiong[a], Xiang Li[a,*]

[a] *School of Environmental and Chemical Engineering, Guangdong Provincial Key Laboratory of Environmental Health and Land Resource, Zhaoqing University, 526061 Zhaoqing, China*

[b] *National Engineering Laboratory for VOCs Pollution Control Technology and Equipment, Guangdong Provincial Key Laboratory of Atmospheric Environment and Pollution Control, School of Environment and Energy, South China University of Technology, 510006 Guangzhou, China*

*Corresponding author. E-mail: chendongdong@zqu.edu.cn; lixiang@zqu.edu.cn.

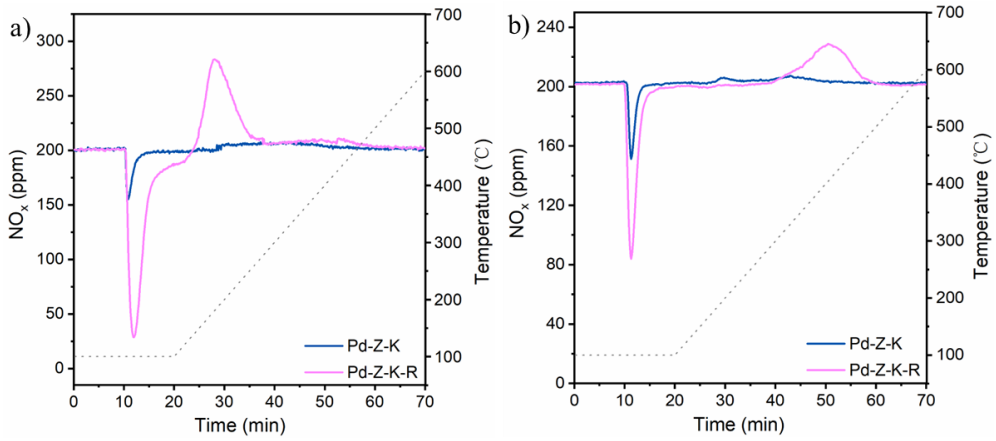

Figure S1. PNA performances of K-poisoned Pd-Z-K and the regenerated Pd-Z-K-R catalysts under different conditions. a) Gas feed: 200 ppm of NO_x and 10 vol.% O_2 in N_2; b) Gas feed: 200 ppm of NO_x, 200 ppm of CO, 3 vol.% H_2O and 10 vol.% O_2 in N_2. Samples were treated at 500 °C in 10 vol% O_2 for one hour before all the tests, and a total flow rate of 200 $mL \cdot min^{-1}$ was used.

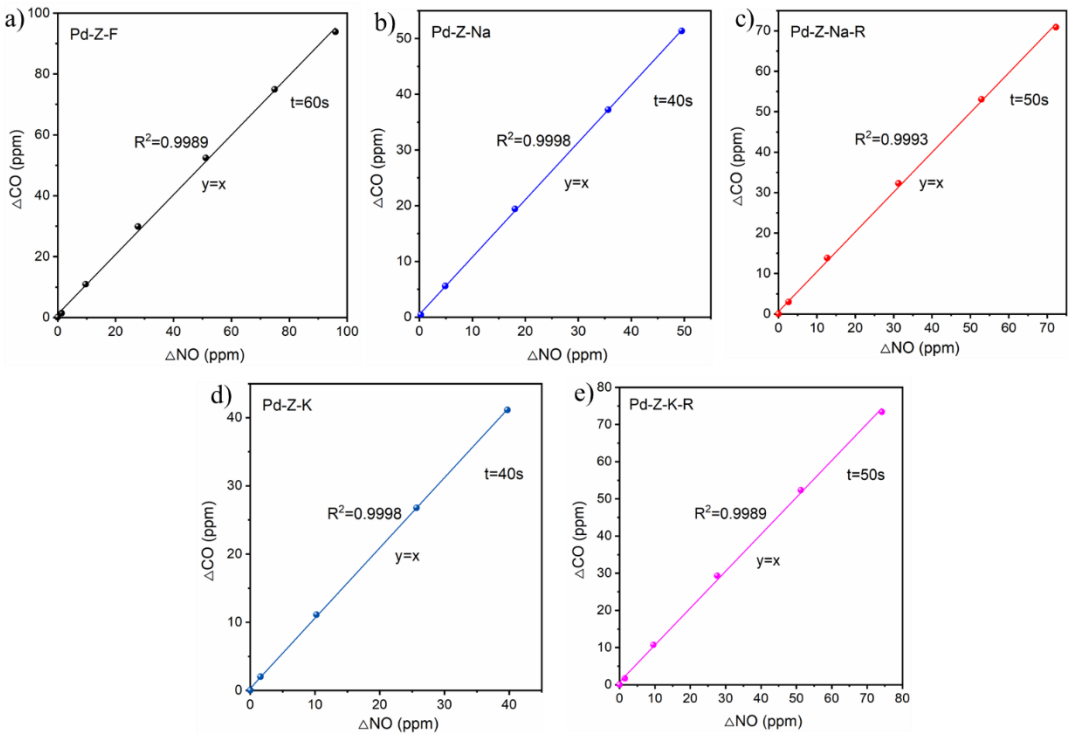

Figure S2. The correlation between the reduced concentrations of NO and CO (labeled as △NO and △CO) during the initial stage of NO_x adsorption in PNA tests over Pd-Z-F (a), alkali-metal poisoned Pd-Z-Na and Pd-Z-K (b and d) and the regenerated Pd-Z-Na and Pd-Z-K catalysts (c and e). △NO (△CO) = C_0 - C_t (C_0 and C_t represent initial and real-time concentrations of NO or CO, respectively). Gas feed: gas feed: 200 ppm of NO_x, 200 ppm of CO, 3 vol.% H_2O and 10 vol.% O_2 in N_2, with a total flow rate of 200 mL min^{-1}. All the samples were pretreated at 500 °C in 10 vol.% O_2 before the tests.

Note: he concentrations of CO and NO exhibited a parallel decline during the initial stages of the PNA test, attributed to the formation of the Pd^{2+}(NO)(CO) intermediate. Notably, a significantly greater quantity of CO and NO is consumed during the PNA tests over Pd-SSZ-13, suggesting the presence of a higher density of isolated Pd^{2+} sites within the material. The introduction of alkali metals leads to a diminution in the number of active Pd^{2+} centers, thereby reducing the formation of the Pd^{2+}(NO)(CO) intermediate. Conversely, regeneration with NH_4Cl solution alleviates the deactivating impact of alkali metals on the Pd sites, resulting in a notably higher production of the Pd^{2+}(NO)(CO) intermediate after washing, in comparison to the poisoned Pd-SSZ-13 catalysts.

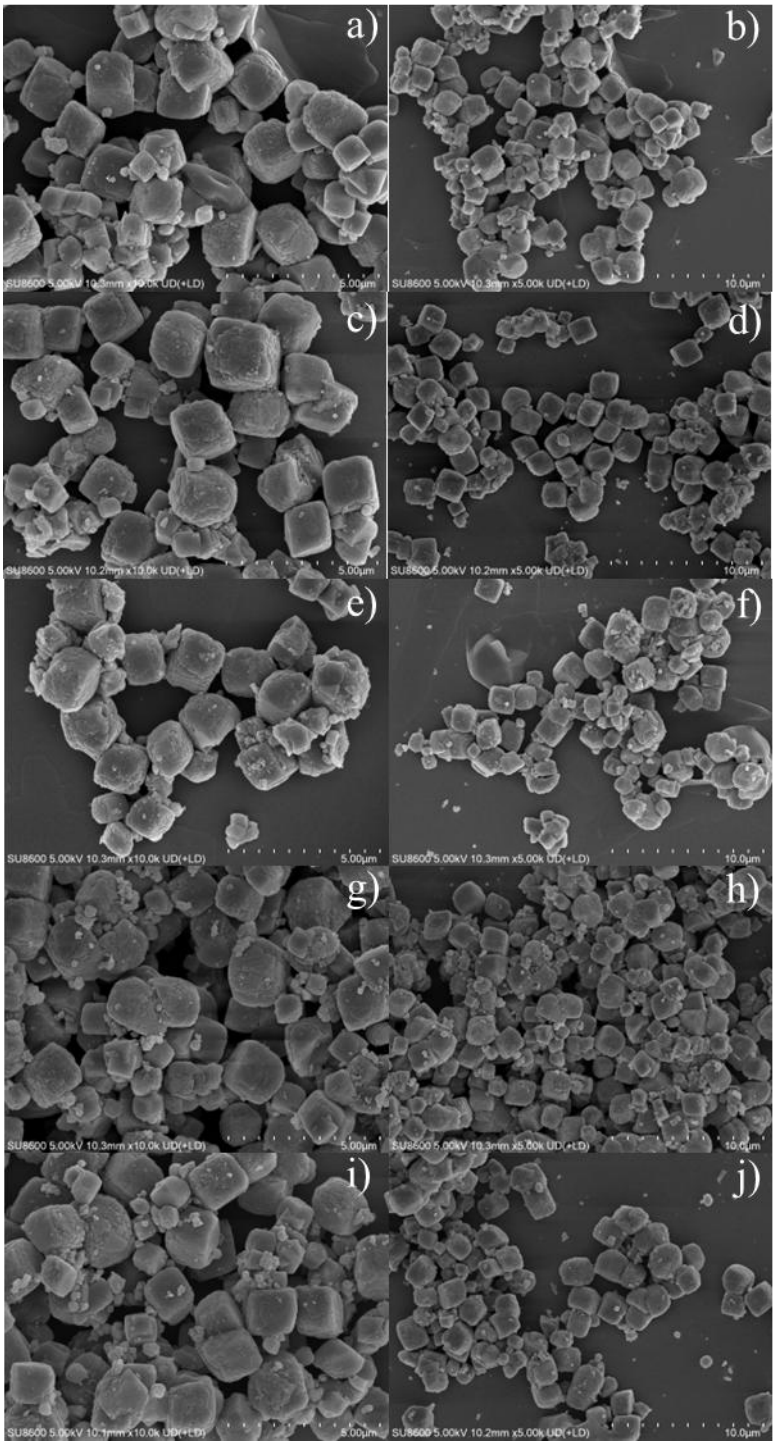

Figure S3. Representative FE-SEM images of Pd-Z-F (a and b), Pd-Z-Na (c and d), Pd-Z-Na-R (e and f), Pd-Z-K (g and h) and Pd-Z-K-R (i and j) catalysts.

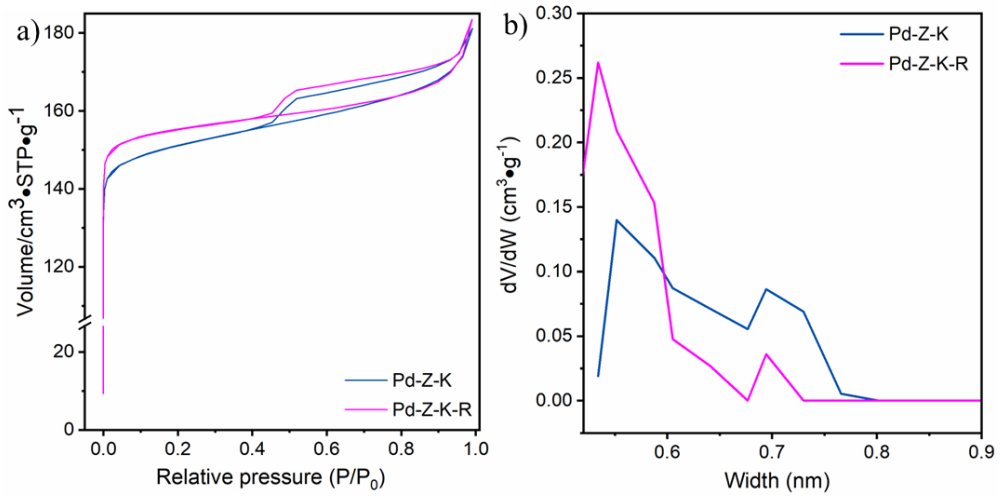

Figure S4. N_2-physisorption curves (a) and micropore size distributions (b) analyzed by the NLDFT method for K-poisoned Pd-Z-K and the regenerated Pd-Z-K-R catalysts.

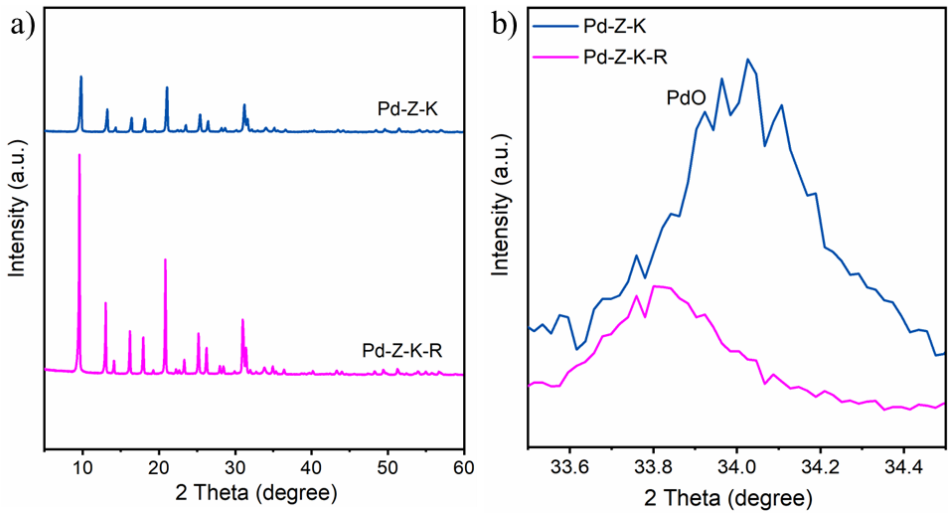

Figure S5. (a) XRD patterns of K-poisoned Pd-Z-K and the regenerated Pd-Z-K-R catalysts. (b) Enlarged XRD patterns (normalized to the intensity of main band at 2θ = 9.6° in the respective spectrum) in 33.5-34.5°.

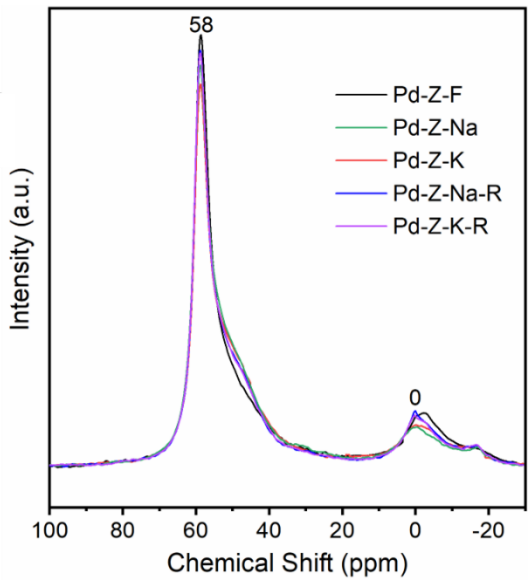

Figure S6. ^{27}Al MAS NMR spectra of fresh, poisoned and regenerated Pd-SSZ-13 catalysts. Pd-Z-F (black), Pd-Z-Na (green), Pd-Z-K (red), Pd-Z-Na-R (blue) and Pd-Z-F (violet).

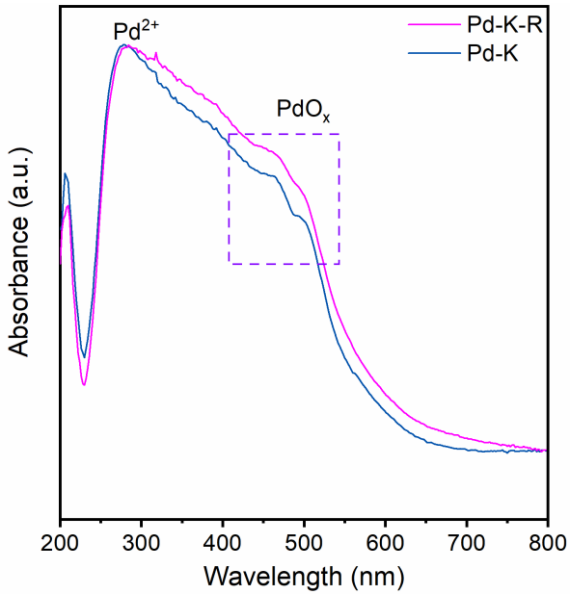

Figure S7. DR UV/Vis spectra of K-poisoned Pd-Z-K and the regenerated Pd-Z-K-R catalysts.

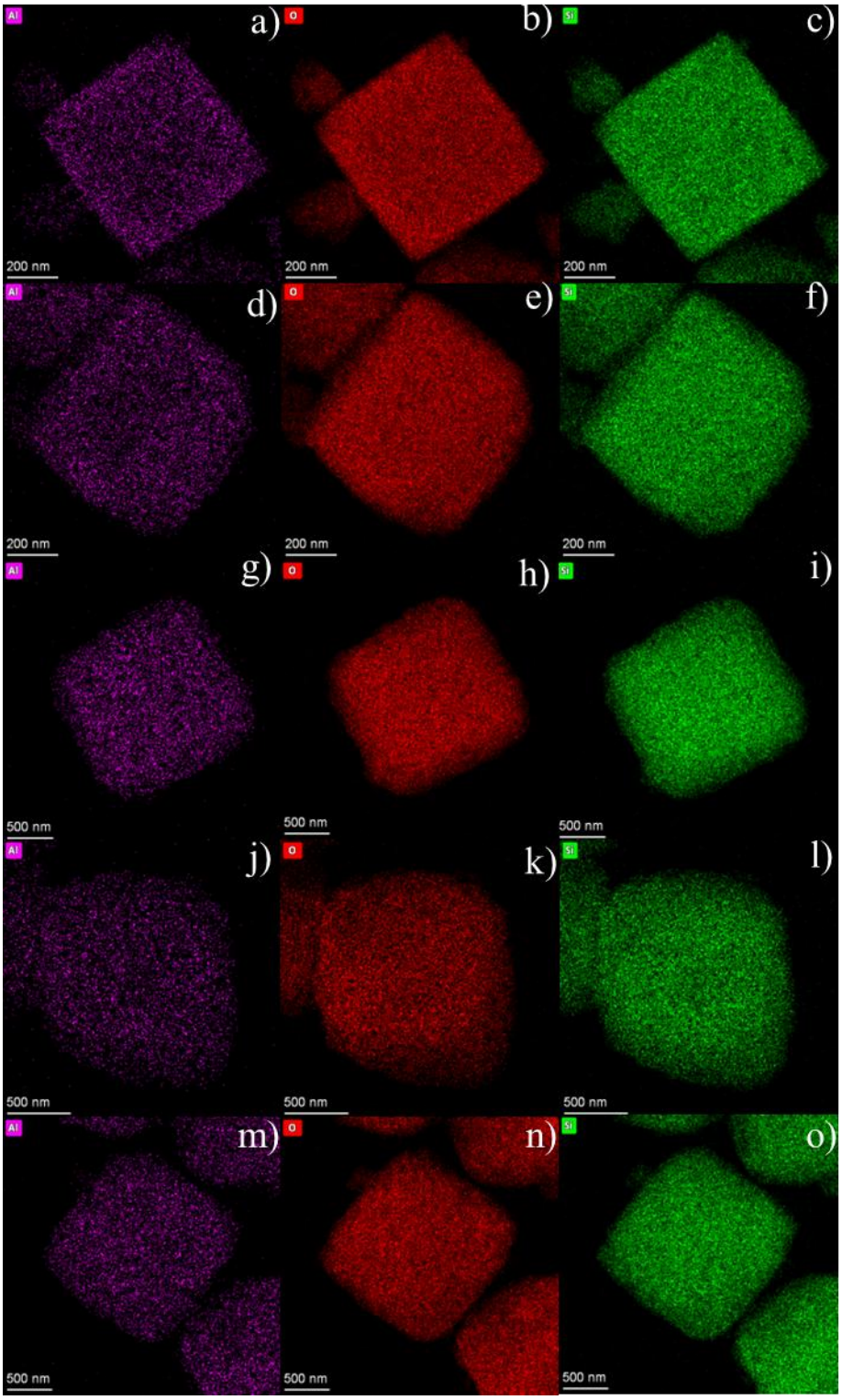

Figure S8. EDX mappings of for Pd-Z-F (panels (a)−(c)), the poisoned Pd-Z-Na (panels (d)−(f)) and Pd-Z-K (panels (g)−(i)), the regenerated Pd-Z-Na-R (panels (j)−(l)) and Pd-Z-K-R (panels (m)−(o)) catalysts.

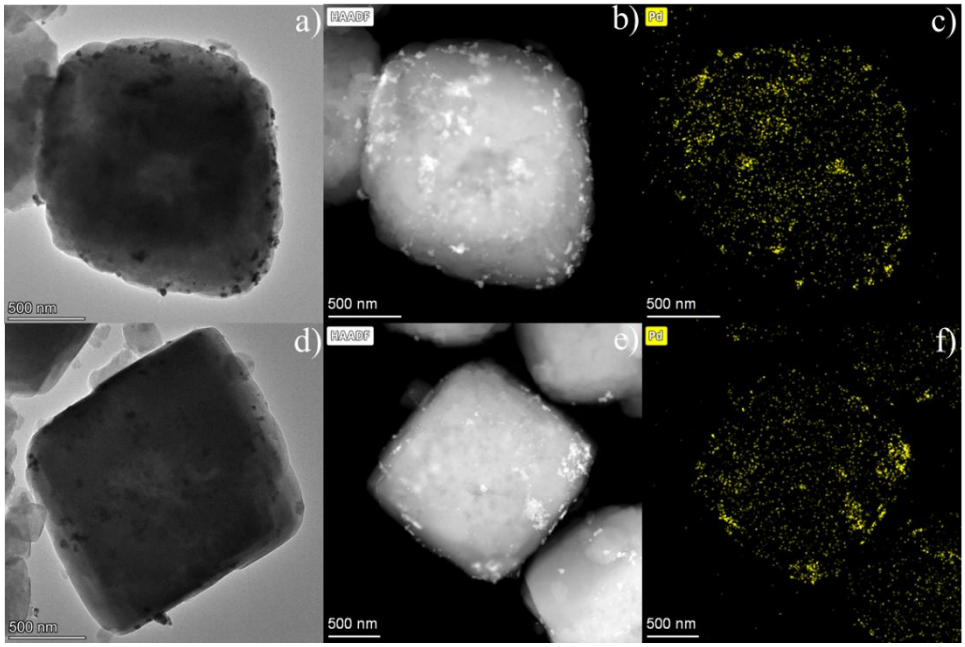

Figure S9. (a, d) TEM, (b, e) HAADF-STEM images, and (c, f) EDX mapping of Pd for Pd-Z-K (panels (a)−(c)) and Pd-Z-K-R (panels (d)−(f)) catalysts.

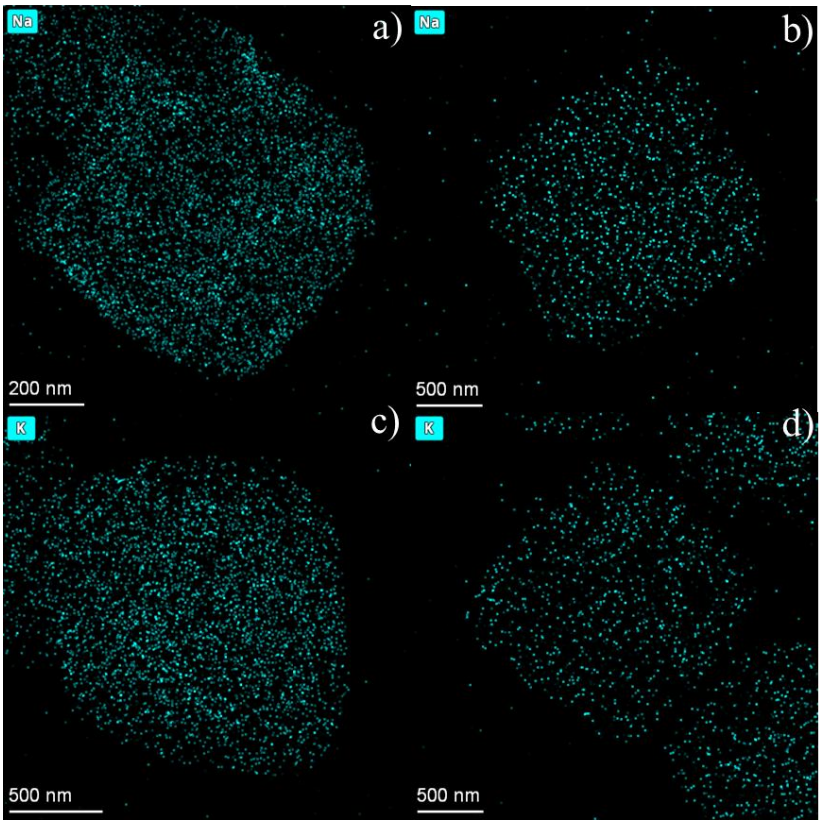

Figure S10. EDX mappings of alkali metals for Pd-Z-Na (a), the regenerated Pd-Z-Na-R (b), Pd-Z-K (C) and the regenerated Pd-Z-K-R (d) catalysts.

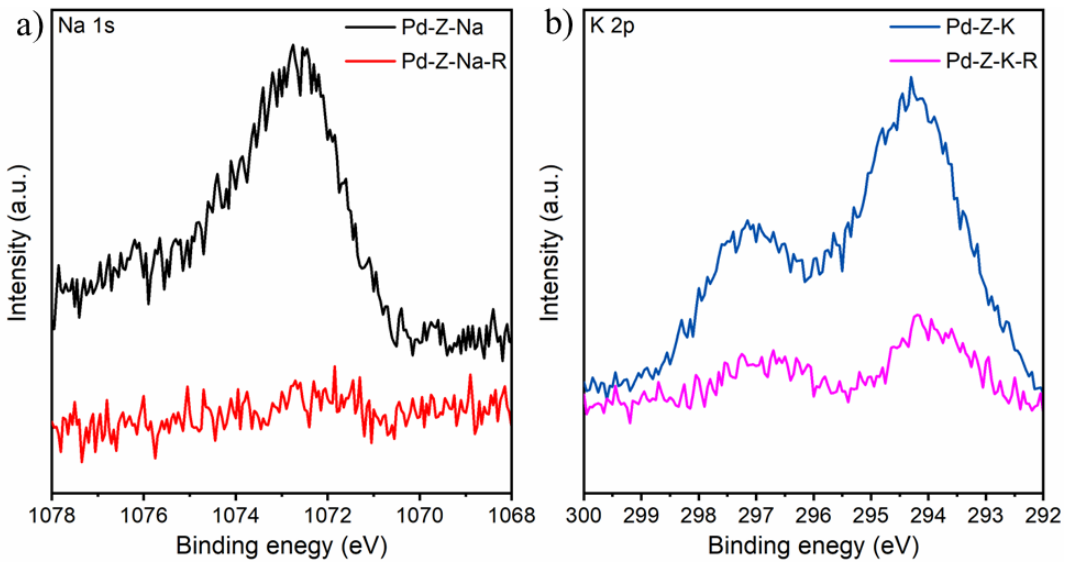

Figure S11. (a) High-resolution XP Na 1s spectra of the poisoned Pd-Z-Na and the regenerated Pd-Z-Na-R catalysts; (b) High-resolution XP K 2p spectra of the poisoned Pd-Z-K and the regenerated Pd-Z-K-R catalysts.

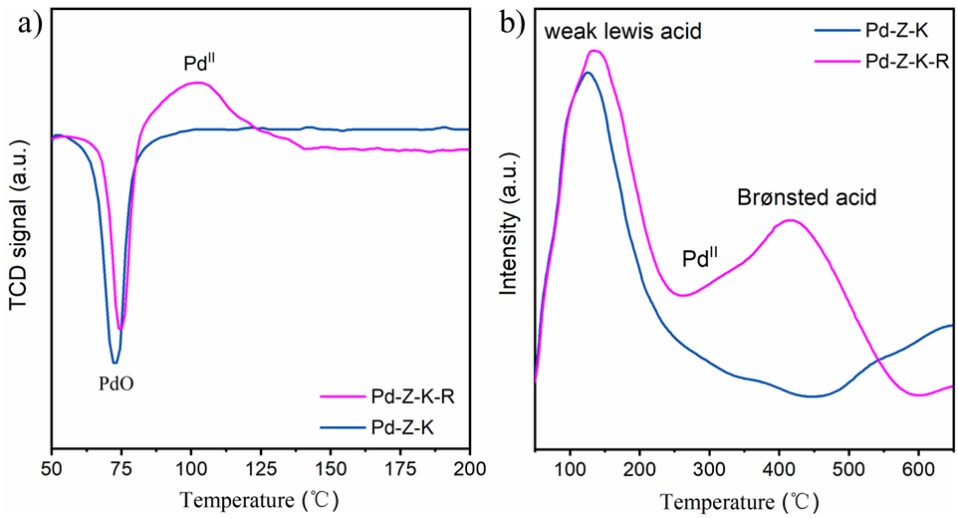

Figure S12. H_2-TPR curves (a) and NH_3-TPD profiles (b) of K-poisoned Pd-Z-K and the regenerated Pd-Z-K-R catalysts.

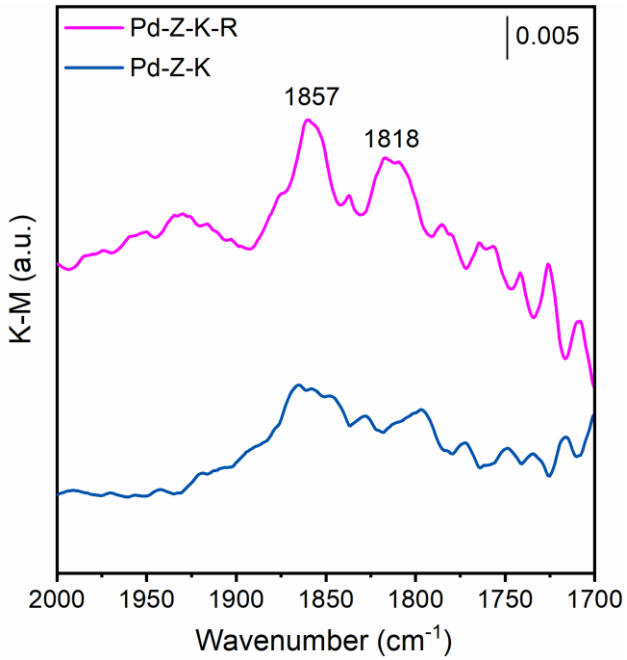

Figure S13. NO-DRIFTS profiles of K-poisoned Pd-Z-K and the regenerated Pd-Z-K-R catalysts.

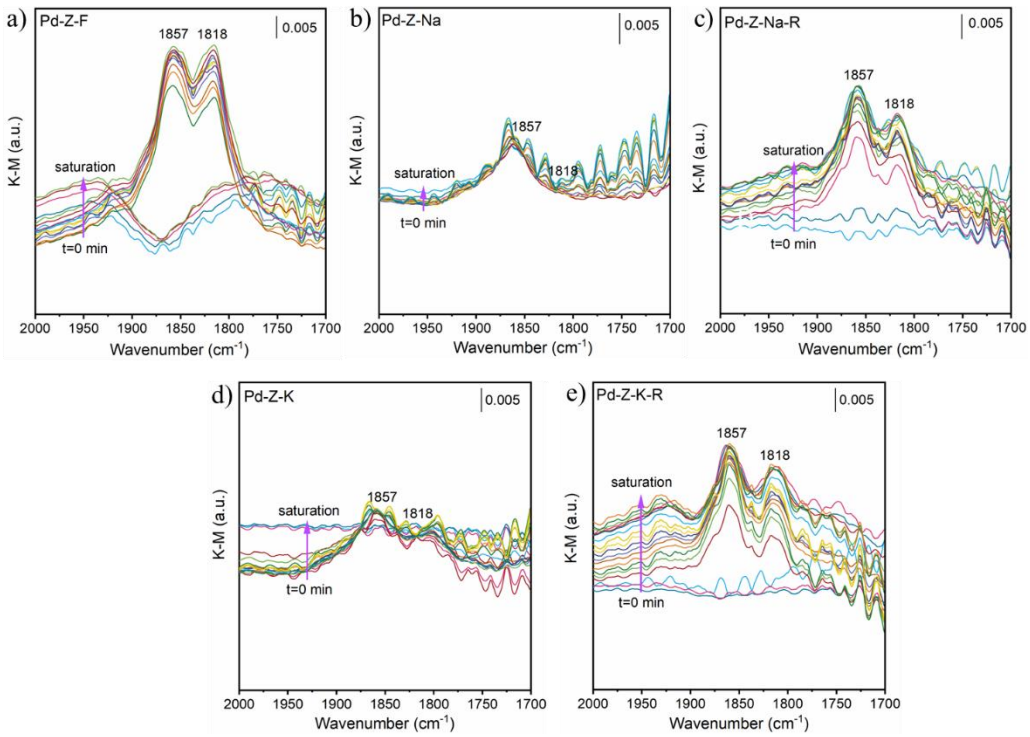

Figure S14. Time-resolved *in situ* NO-DRIFT spectra for the Pd-Z-F(a), alkali-metal poisoned Pd-Z-Na and Pd-Z-K (b and d) and the regenerated Pd-Z-Na-R and Pd-Z-K-R (c and e) catalysts. The measurements were performed at 100 °C after pretreatment in flowing dry air at 500 °C for about 1 h. An initial background spectrum was acquired in a continuous flow of N_2 and subsequently subtracted from all spectra recorded in a NO-enriched atmosphere, all conducted at a consistent temperature of 100 °C.

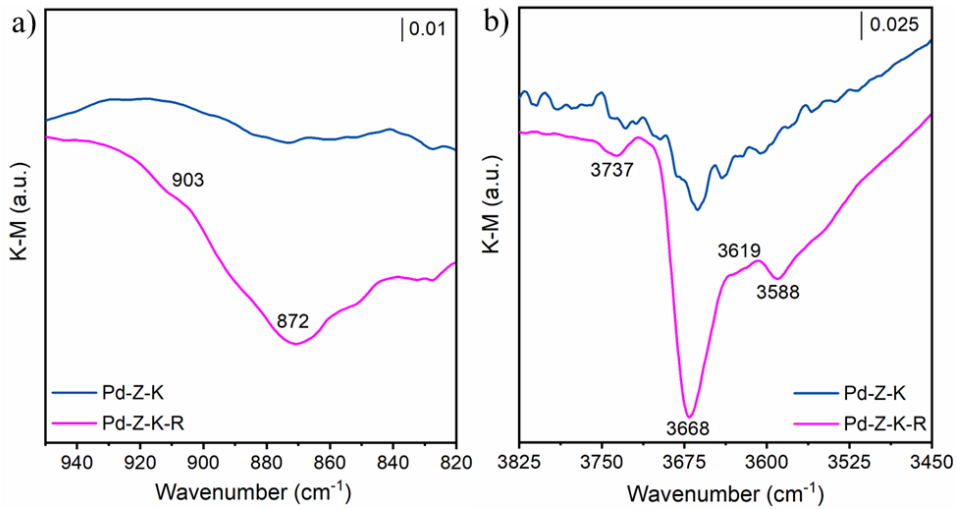

Figure S15. NH_3-DRIFTS profiles of K-poisoned Pd-Z-K and the regenerated Pd-Z-K-R catalysts.

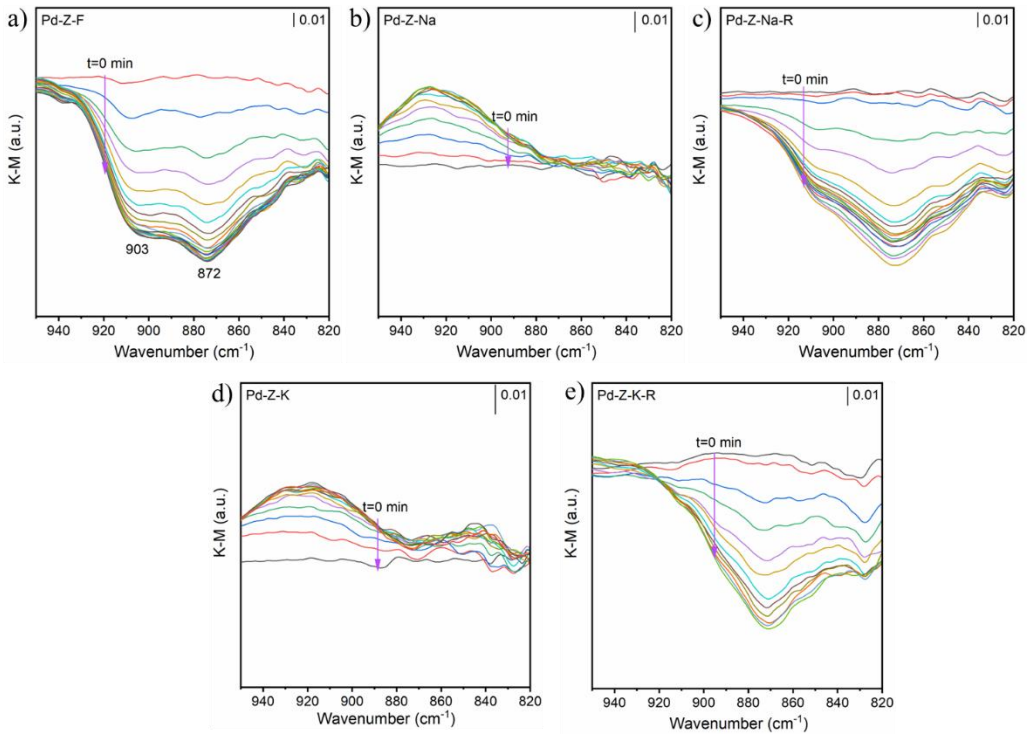

Figure S16. Time-resolved *in situ* NH_3-DRIFT spectra (950-820 cm^{-1}) for the Pd-Z-F(a), alkali-metal poisoned Pd-Z-Na and Pd-Z-K (b and d) and the regenerated Pd-Z-Na-R and Pd-Z-K-R (c and e) catalysts. The measurements were performed at 25 °C after pretreatment in flowing dry air at 500 °C for about 1 h. An initial background spectrum was acquired in a continuous flow of N_2 and subsequently subtracted from all spectra recorded in a NH_3-enriched atmosphere, all conducted at a consistent temperature of 25 °C.

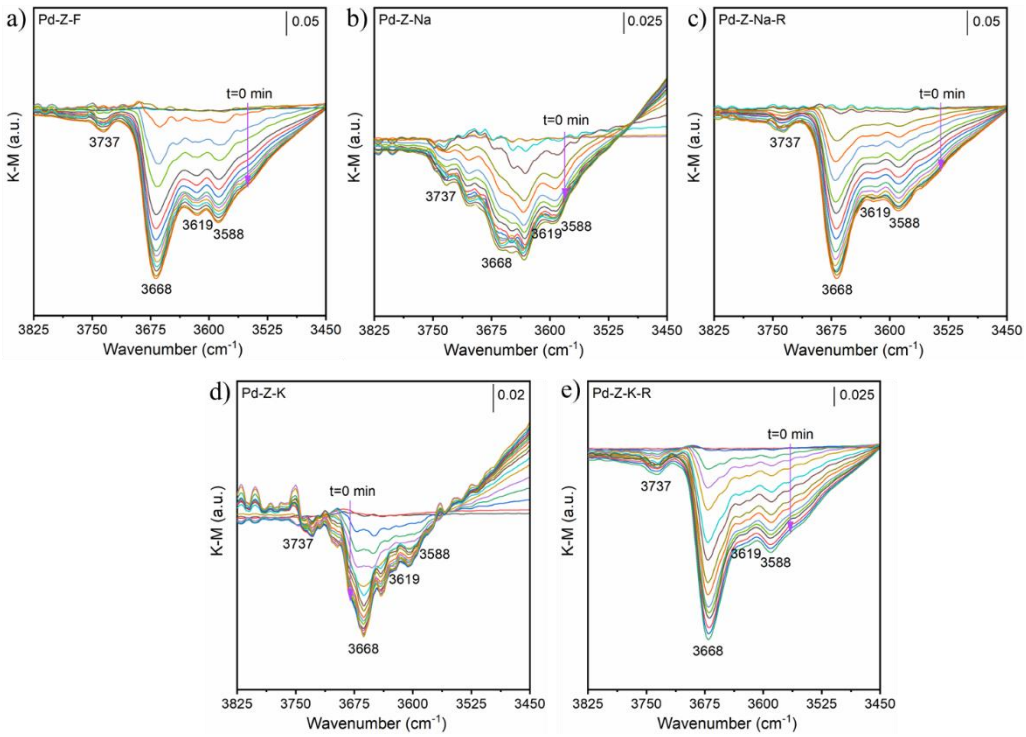

Figure S17. Time-resolved *in situ* NH_3-DRIFT spectra (3825-3450 cm^{-1}) for the Pd-Z-F(a), alkali-metal poisoned Pd-Z-Na and Pd-Z-K (b and d) and the regenerated Pd-Z-Na-R and Pd-Z-K-R (c and e) catalysts. The measurements were performed at 25 °C after pretreatment in flowing dry air at 500 °C for about 1 h. An initial background spectrum was acquired in a continuous flow of N_2 and subsequently subtracted from all spectra recorded in a NH_3-enriched atmosphere, all conducted at a consistent temperature of 25 °C.

Table S1. Textural properties of fresh, alkali-metal-poisoned and Pd-SSZ-13 catalysts.

Sample	S_{BET} ($m^2\ g^{-1}$)	V_{micro} ($cm^3\ g^{-1}$)
Pd-Z-F	536.05	0.233
Pd-Z-Na	497.89	0.205
Pd-Z-K	487.14	0.209
Pd-Z-Na-R	505.74	0.216
Pd-Z-K-R	498.28	0.224

Table S2. Weight percentage of alkali metals before and after NH_4Cl washing determined by ICP-OES.

Sample	Weight (g)	analyte	mass fraction
Pd-Z-Na	0.0405	Na	1.5488%
Pd-Z-Na-R	0.0393	Na	0.1066%
Pd-Z-K	0.0435	K	1.9911%
Pd-Z-K-R	0.0402	K	0.4964%

Table S3. Acid Content (μmol/g) of fresh, alkali-metal-poisoned and Pd-SSZ-13 catalysts Calculated based on Gaussian deconvolution and area integral of the NH_3-TPD curves.

Sample	Weak acid	Moderate acid	Strong acid	total acid
Pd-Z-F	230.2	149.8	134.9	514.9
Pd-Z-Na	194.8	36.5	0	231.3
Pd-Z-K	158.9	28.0	0	186.9
Pd-Z-Na-R	179.3	67.5	126	372.8
Pd-Z-K-R	156.8	62.1	113.2	332.1